@INPROCEEDINGS{cst2014:barb,
AUTHOR = {Barbero, E. J. and Madeo, A. and Zagari, G. and Zinno, R. and Zucco, G.},
TITLE = {A Mixed Finite Element for Static and Buckling Analysis of Laminated Folded Plates},
BOOKTITLE = {The Twelfth International Conference on Computational Structures Technology},
EDITOR = {Topping, B. H. V. and Iv\'anyi, P.},
PUBLISHER = {Civil-Comp Press},
ADDRESS = {Stirlingshire, United Kingdom},
NOTE = {paper 214},
YEAR = 2014,
URL = "http://dx.doi.org/10.4203/ccp.106.214"
}

Paper 214

Proceedings of the Twelfth International Conference
on Computational Structures Technology,
B.H.V. Topping and P. Iványi, (Editors),
Civil-Comp Press, Stirlingshire, Scotland.

A Mixed Finite Element for Static and Buckling Analysis of Laminated Folded Plates

E.J. Barbero[1], A. Madeo[2], G. Zagari[2], R. Zinno[2] and G. Zucco[2]
[1]West Virginia University, Morgantown, United States of America
[2]DIMES, University of Calabria, Rende, Cosenza, Italy

Abstract

A mixed finite element for linear and nonlinear analysis of laminated folded plates is presented in this paper. The mixed formulation affords accurate prediction of stresses, which are needed for damage and failure analysis. Static condensation of the stress parameters results in a displacement-only element that is easy to integrate into commercial packages via their user element feature. The linear element is easily extended for nonlinear analysis by using a corotational formulation. Numerous test cases demonstrate the performance of the element by comparison with existing and, or costlier numerical solutions from the literature. The element is free from spurious modes employing full integration and an incompatible displacement mode on the contour displacements.

Keywords: Laminated folded plates, mixed finite elements, corotational kinematics.

1 Introduction

Laminated composite folded plates are used in many technical fields including pultruded structural shapes in civil engineering, stiffened panels in aerospace structures, etc. Composite materials are used for weight saving, resulting in slender structures that are susceptible to buckling. Open sections are susceptible to buckling mode interaction. Since stiffened panels are edge supported, they are capable of carrying post-critical loads, which must be calculated using costly continuation methods such as the Riks method. Furthermore, a major portion of the computational time is employed in the formulation of the stiffness and geometric stiffness matrices. Therefore, interest in accurate yet computationally inexpensive elements is always desirable.

2 Geometrically linear element

2.1 Geometry

The element is described by four nodes in the X,Y, plane of the global Cartesian coordinate system (c.s.) X, Y, Z. The element midsurface is mapped onto a unit element with midsurface coordinates ξ, η, defined by the nodal coordinates $X_i, Y_i, i = 1, ..., 4$ [1, 2] and

$$
\begin{aligned}
X &= a_0 + a_1\xi + a_2\xi\,\eta + a_3\eta \\
Y &= b_0 + b_1\xi + b_2\xi\,\eta + b_3\eta
\end{aligned}
\tag{1}
$$

In order to cancel the rigid part of the element distortion, a local c.s. x, y is defined by the transformation

$$
\begin{Bmatrix} x \\ y \end{Bmatrix} = \mathbf{R}^T \begin{Bmatrix} X - a_0 \\ Y - b_0 \end{Bmatrix}
\tag{2}
$$

where a_0, b_0, are the coordinates of the element centroid. The rotation matrix is

$$
\mathbf{R} = \begin{bmatrix} \cos\alpha & -\sin\alpha \\ \sin\alpha & \cos\alpha \end{bmatrix}, \qquad \alpha = \arctan\left(\frac{a_3 - b_1}{a_1 + b_3}\right)
\tag{3}
$$

The Jacobian of the coordinate transformation and its average are

$$
\begin{aligned}
\mathbf{J}^G &= \begin{bmatrix} X_{,\xi} & X_{,\eta} \\ Y_{,\xi} & Y_{,\eta} \end{bmatrix} = \begin{bmatrix} (a_1 + a_2\eta) & (a_3 + a_2\xi) \\ (b_1 + b_2\eta) & (b_3 + b_2\xi) \end{bmatrix} \\
\bar{\mathbf{J}}^G &= \frac{1}{4}\int_{\xi=-1}^{1}\int_{\eta=-1}^{1} \mathbf{J}^G \,\mathrm{d}\xi\,\mathrm{d}\eta = \begin{bmatrix} a_1 & a_3 \\ b_1 & b_3 \end{bmatrix}
\end{aligned}
\tag{4}
$$

The average can be decomposed into an orthogonal rotation and a symmetric matrix

$$
\bar{\mathbf{J}}^G = \mathbf{R}\,\bar{\mathbf{J}} \quad ; \quad \bar{\mathbf{J}} = \begin{bmatrix} a & c \\ c & b \end{bmatrix}
$$

2.2 Assumed stress

The stress resultants **t** can be written in terms of eighteen stress parameters $\boldsymbol{\beta}_e$, including nine $\boldsymbol{\beta}_m$ and nine $\boldsymbol{\beta}_f$, as follows

$$
\mathbf{t} = \mathbf{B}\boldsymbol{\beta}_e = \begin{bmatrix} \mathbf{B}_m & 0 \\ 0 & \mathbf{B}_f \end{bmatrix} \begin{Bmatrix} \boldsymbol{\beta}_m \\ \boldsymbol{\beta}_f \end{Bmatrix}
\tag{5}
$$

The 18 parameters correspond to the deformation modes of the element, that is, 24 degrees of freedom (dof) minus 6 rigid body motions. Since the stress field satisfies the equations of equilibrium in the element, i.e., the stresses are self equilibrating, then, the stress resultants **t** can be written in terms known *shape* functions $\mathbf{B}_m, \mathbf{B}_f$ as follows.

Membrane:

$$\mathbf{B}_m = \begin{bmatrix} 1 & 0 & 0 & y & 0 & x & 0 & y^2 & -2\,a^2\,x\,y \\ 0 & 1 & 0 & 0 & x & 0 & y & -x^2 & 2\,b^2\,x\,y \\ 0 & 0 & 1 & 0 & 0 & -y & -x & 0 & a^2\,y^2 - b^2\,x^2 \end{bmatrix}_{3\times 9} \tag{6}$$

Flexural (first three rows) and intralaminar (last two rows):

$$\mathbf{B}_f = \left[\frac{\mathbf{B}_b}{\mathbf{B}_s}\right] = \left[\begin{array}{ccccccccc} 1 & 0 & 0 & x & 0 & y & 0 & x\,y & 0 \\ 0 & 1 & 0 & 0 & x & 0 & y & 0 & x\,y \\ 0 & 0 & 1 & 0 & y\,\bar{c} & x/\bar{c} & 0 & 0 & 0 \\ \hline 0 & 0 & 0 & -1 & -\bar{c} & 0 & 0 & -y & 0 \\ 0 & 0 & 0 & 0 & 0 & -1/\bar{c} & -1 & 0 & -x \end{array}\right]_{5\times 9} \tag{7}$$

with $\bar{c} = a^2/b^2$.

2.3 Assumed displacements

Since the stresses are self equilibrating, the internal work can be computed as a contour integral. Therefore, the displacements need to be interpolated only along the contour. A one-dimensional c.s. $-1 \leq \zeta \leq 1$ is defined along each straight side of the element.

For each element side Γ_k connecting nodes i and j counterclockwise, we define the following quantities.

The midpoint on the side:

$$\Xi_k = \begin{bmatrix} \Xi_{kx} \\ \Xi_{ky} \end{bmatrix} = \frac{1}{2} \begin{bmatrix} x_j + x_i \\ y_j + y_i \end{bmatrix} \tag{8}$$

One half the length of the side:

$$\Delta_k = \begin{bmatrix} \Delta_{kx} \\ \Delta_{ky} \end{bmatrix} = \frac{1}{2} \begin{bmatrix} x_j - x_i \\ y_j - y_i \end{bmatrix} \tag{9}$$

The normal to the side:

$$\mathbf{n}_k = \begin{bmatrix} n_{kx} \\ n_{ky} \end{bmatrix} = \frac{2}{L_k} \begin{bmatrix} \Delta_{ky} \\ -\Delta_{kx} \end{bmatrix} \tag{10}$$

with $L_k = 2\sqrt{\Delta_{kx}^2 + \Delta_{ky}^2}$ being the side length. Using a one-dimensional coordinate $-1 \leq \zeta \leq 1$ along Γ_k, points along the element side are located as

$$x = \Xi_{kx} + \Delta_{kx}\,\zeta \quad , \quad y = \Xi_{ky} + \Delta_{ky}\,\zeta \tag{11}$$

Then, the side displacements are approximated as

$$\mathbf{u}_k(\zeta) = \mathbf{u}_k^{(l)}(\zeta) + \mathbf{u}_k^{(q)}(\zeta) + \mathbf{u}_k^{(c)}(\zeta) \tag{12}$$

where k is the side number. The first term is linear in the nodal displacements u^i, u^j, where i, j are the end nodes of side k

$$\mathbf{u}_k^{(l)}(\zeta) = \frac{1}{2}\{(1-\zeta)\mathbf{u}^i + (1+\zeta)\mathbf{u}^j\}_{3\times 1} \tag{13}$$
$$\text{with } \mathbf{u}^i = \{u_x^i,\, u_y^i,\, u_z^i\}^T, \quad \mathbf{u}^j = \{u_x^j,\, u_y^j,\, u_z^j\}^T$$

where the subscript 3×1 indicates the size of the array. The linear part of the displacement is continuous across the element boundary. The second term is quadratic and also continuous across the element boundary

$$\mathbf{u}_k^{(q)}(\zeta) = \frac{1}{8}\, L_k(\zeta^2 - 1) \begin{Bmatrix} (\varphi_z^i - \varphi_z^j)\, \mathbf{n}_k \\ -(\boldsymbol{\varphi}^i - \boldsymbol{\varphi}^j)^T \cdot \mathbf{n}_k \end{Bmatrix}_{3\times 1} \tag{14}$$

where

$$\boldsymbol{\varphi}^i = \{\varphi_x^i,\, \varphi_y^i\}^T \quad , \quad \boldsymbol{\varphi}^j = \{\varphi_x^j,\, \varphi_y^j\}^T \tag{15}$$

The third term is cubic and incompatible (to prevent rank defectiveness)

$$\mathbf{u}_k^{(c)}(\zeta) = \frac{\theta}{4}\, L_k(\zeta - \zeta^3) \begin{Bmatrix} \mathbf{n}_k \\ 0 \end{Bmatrix}_{3\times 1} \tag{16}$$

where θ is the average in-plane distortional rotation defined as

$$\theta = \frac{1}{4}\sum_{i=1}^{4} \varphi_z^i - \bar{\varphi}_z \tag{17}$$

where $i = 1...4$ are the nodes of the element and $\bar{\varphi}_z$ is the average in-plane rigid rotation calculated as

$$\bar{\varphi}_z = \mathbf{N}_\theta \mathbf{u}_{em} \tag{18}$$

$$\mathbf{N}_\theta = \frac{1}{2\Omega_e}\,[-\Delta_{4y}, \Delta_{4x}, 0, -\Delta_{1y}, \Delta_{1x}, 0, -\Delta_{2y}, \Delta_{2x}, 0, -\Delta_{3y}, \Delta_{3x}, 0] \tag{19}$$

where with $\mathbf{u}_{em} = \{u_{xi}, u_{yi}, \varphi_{zi}...\}^T$ collecting the membrane displacements at the nodes $i = 1...4$. The rest of the displacements, $\mathbf{u}_{ef} = \{u_{zi}, \varphi_{xi}, \varphi_{yi}, ...\}^T$ collect the displacements associated to flexural and intralaminar shear at the nodes. The vectors $\mathbf{u}_{em}$ and $\mathbf{u}_{ef}$ represent nodal displacements/rotations describing membrane and flexural behavior, respectively. Finally, bending rotations at the element side are interpolated linearly, as follows

$$\boldsymbol{\varphi}_k(\zeta) = \frac{1}{2}[(1-\zeta)\boldsymbol{\varphi}_i + (1+\zeta)\boldsymbol{\varphi}_j] \quad \text{with} \quad \boldsymbol{\varphi}_i = \{\varphi_x, \varphi_y\}^T \tag{20}$$

2.4 Mixed element

The Hellinger-Reissner strain energy can be written as

$$\Phi(\mathbf{t},\mathbf{u}) = \int_\Omega \left(\mathbf{t}^T\mathbf{D}\mathbf{u} - \frac{1}{2}\mathbf{t}^T\mathbf{S}\mathbf{t} \right) \mathrm{d}\Omega \tag{21}$$

where

$$\mathbf{t} = \begin{Bmatrix} \mathbf{t}_m \\ \mathbf{t}_f \end{Bmatrix}, \quad \mathbf{u} = \begin{Bmatrix} \mathbf{u}_m \\ \mathbf{u}_f \end{Bmatrix}, \quad \mathbf{D} = \begin{bmatrix} \mathbf{D}_m & \mathbf{0} \\ \mathbf{0} & \mathbf{D}_f \end{bmatrix} \tag{22}$$

where the vectors $\mathbf{t}_m$ and $\mathbf{t}_f$ are the membrane stress resultants, and the moment and shear resultants, respectively; $\mathbf{u}_m$ and $\mathbf{u}_f$ are the in- and out-plane kinematical parameters, defined as follows

$$\mathbf{t}_m = \begin{Bmatrix} N_x \\ N_y \\ N_{xy} \end{Bmatrix} \quad , \quad \mathbf{t}_f = \begin{Bmatrix} M_x \\ M_y \\ M_{xy} \\ V_x \\ V_y \end{Bmatrix} \quad , \quad \mathbf{u}_m = \begin{Bmatrix} u_x \\ u_y \end{Bmatrix} \quad , \quad \mathbf{u}_f = \begin{Bmatrix} u_z \\ \varphi_x \\ \varphi_y \end{Bmatrix} \tag{23}$$

where $\mathbf{N}, \mathbf{M}, \mathbf{V}$ are the membrane, bending, and shear stress resultants, respectively; $\mathbf{u}, \boldsymbol{\varphi}$ are the midsurface strains and rotations, respectively. The corresponding nodal displacements for nodes $i = 1...4$ are

$$\mathbf{u}_{em} = \begin{Bmatrix} u_{xi} \\ u_{yi} \\ \varphi_{zi} \end{Bmatrix}_{12\times1} \quad , \quad \mathbf{u}_{ef} = \begin{Bmatrix} u_{zi} \\ \varphi_{xi} \\ \varphi_{yi} \end{Bmatrix}_{12\times1} \quad , \quad i = 1...4 \tag{24}$$

and the corresponding displacements at any point ζ on side k along the contour

$$\mathbf{u}_{km}(\zeta) = \begin{Bmatrix} u_{xk} \\ u_{yk} \end{Bmatrix}_{2\times1} , \quad \mathbf{u}_{kf} = \begin{Bmatrix} u_{zk} \\ \varphi_{xk} \\ \varphi_{yk} \end{Bmatrix}_{3\times1} , \quad k = \text{fixed}, \quad -1 \leq \zeta \leq 1 \tag{25}$$

The strain-displacement differential operators $\mathbf{D}_m$ and $\mathbf{D}_f$ for first order shear deformation (FSDT) kinematics are defined as

$$\mathbf{D}_m = \begin{bmatrix} \partial/\partial x & 0 \\ 0 & \partial/\partial y \\ \partial/\partial y & \partial/\partial x \end{bmatrix} \quad , \quad \mathbf{D}_f = \begin{bmatrix} 0 & 0 & -\partial/\partial x \\ 0 & \partial/\partial y & 0 \\ 0 & \partial/\partial x & -\partial/\partial y \\ \partial/\partial x & 0 & 1 \\ \partial/\partial y & -1 & 0 \end{bmatrix} \tag{26}$$

The 8×8 stiffness matrix $\mathbf{E}$ and compliance matrix $\mathbf{S} = \mathbf{E}^{-1}$ can be written as

$$\mathbf{E} = \begin{bmatrix} \mathbf{E}_m & \mathbf{E}_{mf} & 0 \\ \mathbf{E}_{mf}^T & \mathbf{E}_f & 0 \\ 0 & 0 & \mathbf{E}_s \end{bmatrix} \quad , \quad \mathbf{S} = \begin{bmatrix} \mathbf{S}_m & \mathbf{S}_{mf} & 0 \\ \mathbf{S}_{mf}^T & \mathbf{S}_f & 0 \\ 0 & 0 & \mathbf{S}_s \end{bmatrix} \tag{27}$$

where $\mathbf{S}_m, \mathbf{S}_{mf}, \mathbf{S}_f, \mathbf{S}_s$ are called α, β, γ, h in [3, Eq. (6.20)]. Note that $\mathbf{S} = \mathbf{E}^{-1}$ and $\mathbf{S}_s = \mathbf{E}_s^{-1}$, but $\mathbf{S}_m \neq \mathbf{E}_m^{-1}$, and so on.

Since the stresses satisfy equilibrium

$$\int_\Omega \mathbf{t}^T \mathbf{D} \mathbf{u} \, \mathrm{d}\Omega = \int_\Gamma \mathbf{t}^T \mathbf{N}^T \mathbf{u} \, \mathrm{d}\Gamma = \int_\Gamma \mathbf{t}_m^T \mathbf{N}_m^T \mathbf{u}_m \, \mathrm{d}\Gamma + \int_\Gamma \mathbf{t}_f^T \mathbf{N}_f^T \mathbf{u}_f \, \mathrm{d}\Gamma \tag{28}$$

where the matrix

$$\mathbf{N} = \begin{bmatrix} \mathbf{N}_m & \mathbf{0} \\ \mathbf{0} & \mathbf{N}_f \end{bmatrix} \tag{29}$$

contains the membrane $\mathbf{N}_m$ and bending $\mathbf{N}_f$ components of the outward unit normal to the contour.

Both the displacements $\mathbf{u}$ and tractions $\mathbf{t}$ are discretized on terms of shape functions

$$\mathbf{t} = \mathbf{B} \, \boldsymbol{\beta}_e, \quad \mathbf{u} = \mathbf{U} \, \mathbf{u}_e \tag{30}$$

where $\mathbf{B}$ is given by (6)–(7) and $\mathbf{U}$ is implicity given by (13)–(16). Then, performing the integration (21) we get

$$\Phi_e = \boldsymbol{\beta}_e^T \mathbf{Q}_e \mathbf{u}_e - \frac{1}{2} \boldsymbol{\beta}_e^T \mathbf{H}_e \boldsymbol{\beta}_e \tag{31}$$

where $\mathbf{D}_e$, $\mathbf{H}_e$, are the kinematics and compliance matrix of the element, respectively. The compliance matrix can be written as follows

$$\mathbf{H}_e = \int_{\Omega_e} \mathbf{B}^T \, \mathbf{S} \, \mathbf{B} \, \mathrm{d}\Omega = \begin{bmatrix} \mathbf{H}_m & \mathbf{H}_{mb} \\ sym & \mathbf{H}_b + \mathbf{H}_s \end{bmatrix} \tag{32}$$

where

$$\begin{aligned} \mathbf{H}_m &= \int_{\Omega_e} \left\{ \mathbf{B}_m^T \mathbf{S}_m \mathbf{B}_m \right\} \mathrm{d}\Omega, \quad \mathbf{H}_{mb} = \int_{\Omega_e} \left\{ \mathbf{B}_m^T \mathbf{S}_{mb} \mathbf{B}_b \right\} \mathrm{d}\Omega \\ \mathbf{H}_b &= \int_{\Omega_e} \left\{ \mathbf{B}_b^T \mathbf{S}_b \mathbf{B}_b \right\} \mathrm{d}\Omega_e, \quad \mathbf{H}_s = \int_{\Omega_e} \left\{ \mathbf{B}_s^T \mathbf{S}_s \mathbf{B}_s \right\} \mathrm{d}\Omega_e \end{aligned} \tag{33}$$

and $\mathbf{B}_m, \mathbf{B}_b, \mathbf{B}_s$ are given by (6)–(7).

Using (28), the kinematics matrix is evaluated through contour integration

$$\mathbf{Q}_e = \int_{\Omega_e} \mathbf{B}^T \, \mathbf{D} \, \mathbf{U} \, \mathrm{d}\Omega_e = \int_{\Gamma_e} \mathbf{B}^T \, \mathbf{N}^T \, \mathbf{U} \, \mathrm{d}\Gamma_e \tag{34}$$

where the contour integral can be broken into four sides $k = 1...4$ as follows

$$\mathbf{Q}_e = \begin{bmatrix} \mathbf{Q}_m & \mathbf{0} \\ \mathbf{0} & \mathbf{Q}_f \end{bmatrix}, \quad \mathbf{Q}_m = \sum_{k=1}^{4} \mathbf{Q}_{mk}, \quad \mathbf{Q}_f = \sum_{k=1}^{4} \mathbf{Q}_{fk} \tag{35}$$

where $\mathbf{Q}_{mk}$ and $\mathbf{Q}_{fk}$ are both 9×12 matrices, defined by the following equations

$$\boldsymbol{\beta}_m^T \mathbf{Q}_{mk} \mathbf{u}_{em} = \int_{-1}^{1} \mathbf{t}_{mk}^T(\zeta)\, \mathbf{N}_{mk}^T\, \mathbf{u}_{mk}(\zeta)\, \mathrm{d}\zeta$$

$$\boldsymbol{\beta}_f^T \mathbf{Q}_{fk} \mathbf{u}_{ef} = \int_{-1}^{1} \mathbf{t}_{fk}^T(\zeta)\, \mathbf{N}_{fk}^T\, \mathbf{u}_{fk}(\zeta)\, \mathrm{d}\zeta \tag{36}$$

with the components of the unit normal to the element side are written as follows as follows

$$\mathbf{N}_{mk} = \begin{bmatrix} n_{kx} & 0 & n_{ky} \\ 0 & n_{ky} & n_{kx} \end{bmatrix}, \quad \mathbf{N}_{fk} = \begin{bmatrix} 0 & 0 & 0 & n_{kx} & n_{ky} \\ n_{kx} & n_{ky} & 0 & 0 & 0 \\ -n_{ky} & 0 & -n_{kx} & 0 & 0 \end{bmatrix} \tag{37}$$

or

$$\mathbf{Q}_m = \sum_{k=1}^{4} \int_{-1}^{1} \mathbf{B}_{mk}^T\, \mathbf{N}_{mk}^T\, \mathbf{U}_{mk}\, \mathrm{d}\zeta$$

$$\mathbf{Q}_f = \sum_{k=1}^{4} \int_{-1}^{1} \mathbf{B}_{fk}^T\, \mathbf{N}_{fk}^T\, \mathbf{U}_{fk}\, \mathrm{d}\zeta \tag{38}$$

where $\mathbf{B}_{mk}$ and $\mathbf{B}_{fk}$ correspond to $\mathbf{B}_m$ and $\mathbf{B}_f$ evaluated on the side k while $\mathbf{U}_{mk}$ and $\mathbf{U}_{fk}$ are defined as

$$\mathbf{U}_{mk} = \frac{\partial \mathbf{u}_{mk}}{\partial \mathbf{u}_{em}}, \quad \mathbf{U}_{fk} = \frac{\partial \mathbf{u}_{fk}}{\partial \mathbf{u}_{ef}} \tag{39}$$

In particular, for side $k = 1$ (nodes $i = 1$ and $j = 2$), we have

$$\mathbf{U}_{m1} = \left[\begin{matrix} \frac{1-\zeta}{2} - \frac{L_k\, n_{kx}\, \Delta_{4y}(\zeta-\zeta^3)}{8\,\Omega_e} & 0 & \frac{n_{kx}(\zeta^2-1)}{8\,L_k} \\ 0 & \frac{1-\zeta}{2} + \frac{L_k\, n_{ky}\, \Delta_{4x}(\zeta-\zeta^3)}{8\,\Omega_e} & \frac{n_{ky}(\zeta^2-1)}{8\,L_k} \end{matrix}\right.$$
$$\left.\begin{matrix} \frac{1+\zeta}{2} - \frac{L_k\, n_{kx}\, \Delta_{1y}(\zeta-\zeta^3)}{8\,\Omega_e} & 0 & -\frac{n_{kx}(\zeta^2-1)}{8\,L_k} & 0 & 0 & 0 & 0 & 0 & 0 \\ 0 & \frac{1+\zeta}{2} + \frac{L_k\, n_{ky}\, \Delta_{1x}(\zeta-\zeta^3)}{8\,\Omega_e} & -\frac{n_{ky}(\zeta^2-1)}{8\,L_k} & 0 & 0 & 0 & 0 & 0 & 0 \end{matrix}\right]_{3\times 12} \tag{40}$$

$$\mathbf{U}_{f1} = \begin{bmatrix} \frac{1-\zeta}{2} & -n_{kx} & -n_{ky} & \frac{1+\zeta}{2} & n_{kx} & n_{ky} & 0 & 0 & 0 & 0 & 0 & 0 \\ 0 & \frac{1-\zeta}{2} & 0 & 0 & \frac{1+\zeta}{2} & 0 & 0 & 0 & 0 & 0 & 0 & 0 \\ 0 & 0 & \frac{1-\zeta}{2} & 0 & 0 & \frac{1+\zeta}{2} & 0 & 0 & 0 & 0 & 0 & 0 \end{bmatrix}_{3\times 12} \tag{41}$$

For other sides the contributions can be obtain by an index permutation in Eqs. (40)-(41).

3 Geometrically non-linear element

Using corotational algebra to describe the element rigid body motion, a linear finite element can be easily made into a geometrically nonlinear one [4]. A corotational frame $\{\bar{\mathbf{e}}_1, \bar{\mathbf{e}}_2, \bar{\mathbf{e}}_3\}$ is next defined with respect to the fixed frame $\{\mathbf{e}_1, \mathbf{e}_2, \mathbf{e}_3\}$

$$\bar{\mathbf{e}}_k = \mathbf{Q}(\boldsymbol{\alpha})\mathbf{e}_k, \quad k = 1..3 \tag{42}$$

where the local reference frame is a Cartesian frame $\{\mathbf{e}_1, \mathbf{e}_2, \mathbf{e}_3\}$ defined so that the average Jacobian of the iso–parametric transformation is symmetric. In (42), $\mathbf{Q}$ is a rigid body rotation parametrized by the rotation vector $\boldsymbol{\alpha}$ according to [5] (see Fig. 1 and [6]) with the origin translated by the vector $\mathbf{c}$.

The displacement and the rotation in the corotational frame $\bar{\mathbf{u}}$ and $\bar{\mathbf{R}}$ can be written

$$\bar{\mathbf{u}} = \mathbf{Q}^T(\mathbf{X} + \mathbf{d} - \mathbf{c}) - \mathbf{X} \quad , \quad \bar{\mathbf{R}} = \mathbf{Q}^T\mathbf{R} \tag{43}$$

where $\mathbf{u}, \mathbf{R}$ are the displacement and rotation associated to position $\mathbf{X}$ in the fixed reference frame, respectively. The rotation vectors $\bar{\boldsymbol{\psi}}, \boldsymbol{\psi}$ represent the rotation tensors $\bar{\mathbf{R}}, \mathbf{R}$ with

$$\bar{\boldsymbol{\psi}} = \log(\bar{\mathbf{R}}(\bar{\boldsymbol{\psi}})) = \log\left(\mathbf{Q}^T(\boldsymbol{\alpha})\mathbf{R}(\boldsymbol{\psi})\right) \tag{44}$$

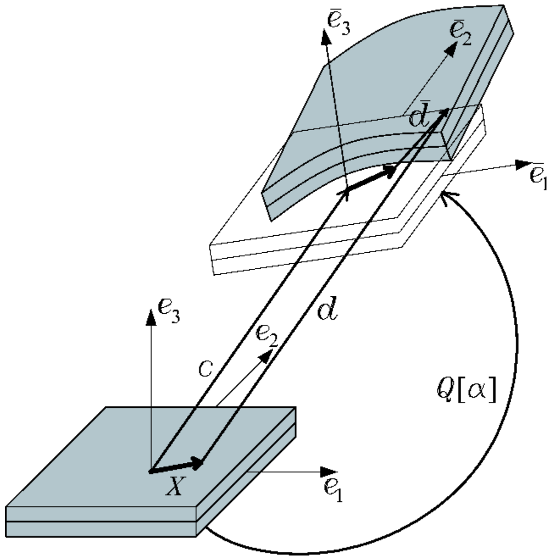

Figure 1: Corotational frame [6].

A corotational frame is defined for each element using the element rotation vector $\boldsymbol{\alpha}_e$ which is a function of the element dof $\mathbf{u}_e$ in the fixed frame

$$\boldsymbol{\alpha}_e = \boldsymbol{\alpha}_e(\mathbf{u}_e) \tag{45}$$

The local dof $\bar{\mathbf{u}}_e$ in the corotational frame are related to $\mathbf{u}_e$ by the geometrical transformation

$$\bar{\mathbf{u}}_e = \mathbf{g}(\mathbf{u}_e) \tag{46}$$

where $\mathbf{g}$ collects the corotational transformations of displacements (43) and rotations (44), rearranged in terms of the definition of local dof $\bar{\mathbf{u}}_e$ of the element.

A linear finite element with energy (21) can be transformed into a geometrically nonlinear element by introducing a corotational description, i.e., referring the element dof in eq. (21) to the corotational frame as follows

$$\Phi_e(\boldsymbol{\beta}_e, \mathbf{u}_e) = \boldsymbol{\beta}_e^T\, \mathbf{D}_e\, \mathbf{g}(\mathbf{u}_e) - \frac{1}{2}\boldsymbol{\beta}_e^T\, \mathbf{H}_e\, \boldsymbol{\beta}_e \tag{47}$$

The element dof can be expressed as

$$\mathbf{u}_e = \{\boldsymbol{\beta}_e,\, \mathbf{u}_e\}^T \tag{48}$$

that collects all the dof in a single vector. The later is related to the global configuration vector $\mathbf{u}_G$ through the standard assemblage procedure

$$\mathbf{u}_e = \mathbf{A}_e \mathbf{u}_G \tag{49}$$

where the matrix $\mathbf{A}_e$ implicitly includes the connectivity constraints between elements. For the Hellinger-Reissner formulation used here, the components of $\mathbf{u}_e$ are the global displacements/rotations of the element nodes plus stress parameters in each element. The stress parameters can be eliminated by static condensation at the element level, leading to a pseudo-compatible system [7].

For nonlinear analysis, the corotational frame is obtained by simply setting the rotation vector equal to the average nodal rotations of element e in the fixed frame, where $i = 1...4$ are the nodes of the element

$$\boldsymbol{\alpha}_e = \frac{1}{4}\sum_{i=1}^{4} \boldsymbol{\varphi}_i \tag{50}$$

4 Results

To illustrate some of the capabilities of the proposed element, the box beam shown in Figure 2 is analyzed (see also [8]) and the predictions compared with CADEC [9] and Abaqus [10]. The side flanges and webs have a width $a = 2.5$ mm and the top flange is $2a$. Two thickness are considered $t/a = 3/10, 1/2$. The ply properties are $E_1 = 104$ GPa; $E_2 = 10.3$ GPa; $G = 5.15$ GPa; $\nu_{12} = 0.21$. The laminate stacking sequence is $[0/90/0/90]$. The column is loaded and simply supported at both ends while the side flanges are free. The load is a uniform edge pressure applied at the column ends on either (a) the skin only, or (b) on both skin and stiffener walls. The buckling loads are shown in Table 1 and Figure 2. Additional results are presented at the conference.

5 Conclusions

Static condensation of the stress dof results in an mixed element with 24 displacement dof that exhibits significantly less computational cost than 48-dof displacement-based elements but with comparable accuracy for the same number of global nodes. Furthermore, the corotational approach significantly simplifies the non-linear computations because the nonlinearity is limited to the corotational mapping.

Lenght $[mm]$	t/a	CADEC	MISS-4 Skin Only	S8R	CADEC	MISS-4 Skin&Stiffener	S8R
				Flange Mode			
20	3/10	9516	10161	9624	16202	16212	15381
20	1/2	22970	24284	23528	35720	36620	35016
			ϕ_y Mode			ϕ_z Mode	
200	3/10	264	256	260	1310	1314	1210
200	1/2	462	444	456	2168	2220	2102

Table 1: Buckling loads (in Newtons) for the box beam loaded axially. The mesh used for the analysis is reported in Fig. 2.

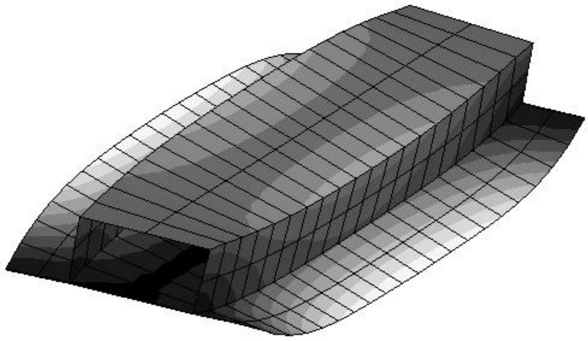

Figure 2: Buckling mode for the box beam loaded axially with uniform edge-pressure and simply supported at both ends on skin only, L=20 mm, a/t=3/10.

6 Acknowledgments

The first author acknowledges the support of the Energy Materials Science and Engineering (EMSE) program at West Virginia University. The remaining authors wish to acknowledge the RISPEISE cooperation project for their financial support.

References

[1] A. Madeo, G. Zagari, R. Casciaro. ”An isostatic quadrilateral membrane finite element with drilling rotations and no spurious modes”, Finite Element in Analysis and Design, 50, 21-32, 2012.

[2] A. Madeo, G. Zagari, R. Casciaro, S. de Miranda, ”A mixed 4-node 3D plate element based on self-equilibrated isostatic stresses”, *accepted for publication International Journal of Structural Stability and Dynamics*, (2013).

[3] E. J. Barbero. ”Introduction to composite materials design–Second Edition”, Boca Raton, FL: CRC Press, 2011.

[4] G. Garcea, A. Madeo, G. Zagari, R. Casciaro. ”Asymptotic post-buckling FEM analysis using corotational formulation”, International Journal of Solids and

Structures, 46, 377-397, 2009.
[5] O. Rodrigues. ”Des lois géométriques qui régissent les déplacements d’un système solide dans l’espace, et de la variation des coordonnées provenant de ces déplacements considérés indépendamment des causes qui peuvent les produire”, Journal de Mathématiques Pures et Appliques, 5, 380-440, 1840.
[6] E.J. Barbero, A. Madeo, G. Zagari, R. Zinno, G. Zucco, ”Koiter asymptotic analysis of folded laminated composite plates”, Composites Part B: Engineering, 61, 267-274, 2014.
[7] A. Bilotta, R. Casciaro. ”Assumed stress formulation of high order quadrilateral elements with an improved in-plane bending behaviour”, Computer Methods in Applied Mechanics and Engineering, 191(15-16), 1523-1540, 2002.
[8] E.J. Barbero, A. Madeo, G. Zagari, R. Zinno, G. Zucco, ”A mixed isostatic 24 dof element for static and buckling analysis of laminated folded plates”, Composite Structures, http://dx.doi.org/10.1016/j.compstruct.2014.05.003, 2014.
[9] http://cadec-online.com/Chapters/Chapter11/Buckling.aspx
[10] Hibbitt, Karlsson, Sorensson. Abaqus theory manual, version 6.8, Dassault 2009.